

COMPUTER SIMULATIONS OF THE DYNAMIC BEHAVIOR OF THREE POINT BEND SPECIMENS

Ouk S. Lee* and Jae Ung Cho**

(Received December 24, 1991)

Computer simulations of the mechanical behavior of a three point bend specimen with a quarter notch under impact load are performed. Two cases with different load application points at the side and at the middle of the specimen are considered. An elastic-plastic von Mises material model is chosen. Three phases such as impact, bouncing and bending phases are found to be identified during the period from the moment of impact to the estimated time for crack initiation. The quasi static case is compared with the above two cases. It is clearly shown that no plastic deformation near the crack tip is appeared at the impact phase. However, it is confirmed that the plastic zone near the crack tip emerges in the second phase and the plastic hinge has been formed in the third phase i.e., at the end of which a quasi static state is reached.

Key Words : Gap Element, Von Mises Material, Impact Phase, Bouncing Phase, Bending Phase, Gap Opening Displacement, Reaction Force, Plastic Zone, Quasi Static State, Crack Mouth Opening Displacement

1. INTRODUCTION

During the development of dynamic fracture mechanics, the notched three point bend specimen has been frequently used. Examples among others are the experimental investigations by Kalthoff (Kalthoff, 1983), Kanninen et al. (Kanninen, 1979), Rosakis et al. (Rosakis, 1988) and van Elst (van Elst, 1984), and the finite element analysis by Ahmad et al. (Ahmad, 1983). In most cases, the experiments were made by using a drop weight to apply the load at the middle point (A in Fig. 2) of the specimen.

The loading velocity that can be obtained by many published methods is believed to be, however, rather limited. In order to widen the understanding of dynamic fracture behavior of structures and materials under high rate of loading, an experimental investigation has been performed using a unique acceleration track with high performance (Wihlborg, 1985). With this equipment, impact velocities from 10 m/s to 60 m/s could be reached (Wihlborg, 1985). For practical purposes, the impact heads hit the side points (B in Fig. 2) instead of the middle point.

In this paper, it is attempted to characterize the dynamic behavior of three point bend specimen with two different kinds of loading arrangement using dynamic finite element method.

2. MATERIAL DESCRIPTION AND FINITE ELEMENT MODEL

The material properties of an isotropic elastic-plastic har-

dening von Mises material is supposed to be the followings. Young's modulus $E=206$ GPa, Poisson's ratio $\nu=0.3$, density $\rho=7800$ Kg/m³ and yield stress $\sigma_y=360$ MPa. The stress to strain curve is shown in Fig. 1, First yield occurs at 360 MPa as shown in Fig. 1. The material then hardens to 1630 MPa, after which it is perfectly plastic. Assuming the Young's modulus is 206 GPa, it can be shown that the plastic strain at the 100 percent strain point is 1. The slope during the linear plastic hardening phase is $E'=1262.2$ MPa until the equivalent von Mises stress reaches 1630 MPa.

The dimensions of the specimen are shown in Fig 2, with the crack length equal to one quarter of the specimen's height. Due to symmetry, only half the specimen is considered and a two-dimensional mesh including 92 eight node plane stress element with reduced integration is chosen. The finite element model is shown in Fig. 3. Reduced integration uses a lower order integration to form the element stiffness; the mass matrix and distributed loadings have been integrated exactly. Reduced integration usually provides more accurate

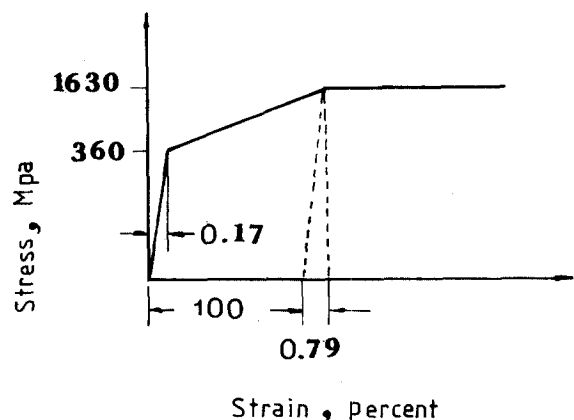


Fig. 1 The material model

*Department of Mechanical Engineering, Inha University, Incheon, 402-751, Korea

**Department of Mechanics, Cheonan Junior Technical College, 275-1, Bu-Dae Dong Cheonan City, Chungnam, 330-240, Korea

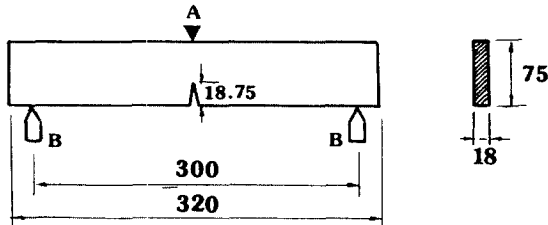


Fig. 2 Three point bend specimen with a quarter notch

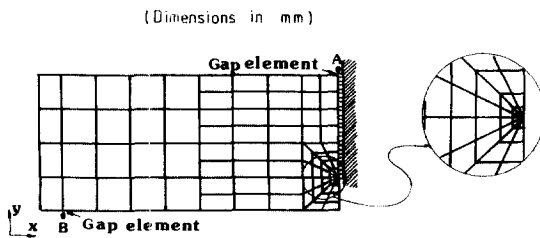


Fig. 3 The finite element model

results with significant reduction of running time. The mesh near the crack tip is concentrated by using degenerated eight node elements as shown in Fig. 3. From experiments (Bergmark, 1991), it was observed that the specimen bounces slightly after impact. In order to model a possible loss of contact at the load and support points, gap elements with one degree of freedom are introduced at the support points A and B (ABAQUS, 1989). Gap elements placed between nodes allow for the nodes to be in contact (gap closed) or separated (gap open) with respect to be in contact and clearance conditions. The used gap element is a unidirectional gap, where contact between the nodes is determined by their relative positions in a fixed direction in space. This seems to be the simplest gap condition. The contact direction (n) is investigated as well as the initial clearance (d) of the bodies are specified on the gap element. This relative displacement in the given direction is defined as;

$r = (u_1 - u_2) * n$ where u_1 is the total displacement at the first node given on the gap element and u_2 is the total displacement at the second node given on the gap element. This direction cosine vector (n) is defined as positive going from the first to the second node of the element. When this relative displacement tries to exceed the initial clearance, the gap is closed and a constraint imposed, so that the element imposes the condition $r \leq d$. If the initial clearance is specified as zero or negative, the gap is initially assumed to close. Gap elements shown in Fig. 3 also provide the reaction force and the gap opening displacement between the specimen and the impact head or support point.

3. BOUNDARY CONDITIONS

The static case, the mechanical behavior of the notched three point bend specimen is, of course, independent of whether the load or displacement is imposed at the middle point or symmetrically at the side points. For the dynamic situation, however, this is not the case since the stress waves are initiated at different points. This implies different stress wave propagation paths towards the crack tip. In order to investigate the phenomena taking place in these two models

and in order to get useful information for the dynamic experiments, a finite element model is used to simulate the procedure and to compare the dynamic behavior of the specimen under the two different boundary conditions.

In the following discussion, models 1 and 2 correspond to load application at the side points B and at the middle point A, respectively. The impact head is assumed to hit the specimen at time zero and its mass is 200 Kg. The impact velocity is chosen as $V = 15$ m/s. This velocity is applied at time zero and is kept constant through the entire calculation. The simulations are performed from the beginning of impact in case of no crack propagation until $600 \mu\text{s}$. In some cases the calculations were extended until $1800 \mu\text{s}$ is reached.

4. COMPARISON OF DYNAMIC RESPONSES BETWEEN TWO MODELS

The deformations and reaction forces at point A and B are calculated during the loading and compared between two models. The development of the plastic zone is investigated until the estimated time for crack initiation. The following notations are used.

F : Force
D : Gap opening displacement

Subscripts ;
1 and 2 : Model 1 and Model 2, respectively
A and B : middle point A and side point B, respectively

For example, the loading force at point B in model 1 is denoted by F_{1B} .

4.1 The Deformation and Reaction Force in Model 1

The reaction forces at the load point B and the support point A and the gap opening displacement at point A are shown in Fig. 4 with respect to time.

F_{1B} is the force at each one of the point B in Fig. 2 and F_{1A} is one half the force at point A. This definition is chosen

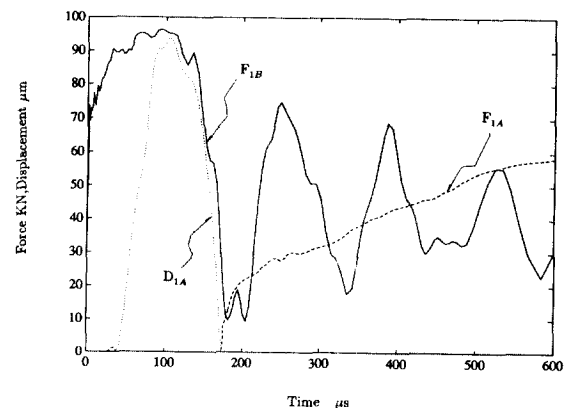


Fig. 4 Dynamic response of model 1, impact at the side point B
Time scale shows the time after impact
 F_{1B} : Reaction force at B (solid line) ;
 F_{1A} : Reaction force at A (dashed line) ;
 D_{1A} : Gap opening displacement at the middle point (dotted line)

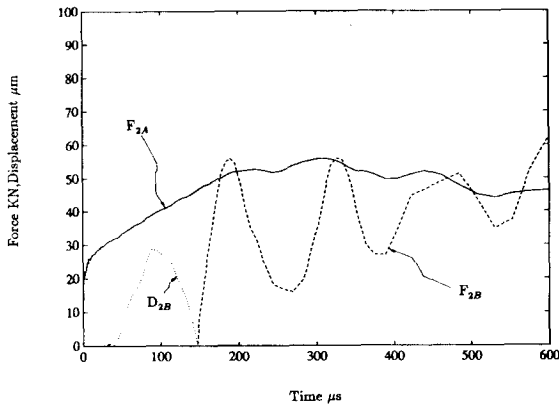


Fig. 5 Dynamic response of model 2, impact at the middle point A
 Time scale shows the time after impact
 F_{2A} : Reaction force at A (solid line) ;
 F_{2B} : Reaction force at B (dashed line) ;
 D_{2B} : Gap opening displacement at the side point (dotted line) ;

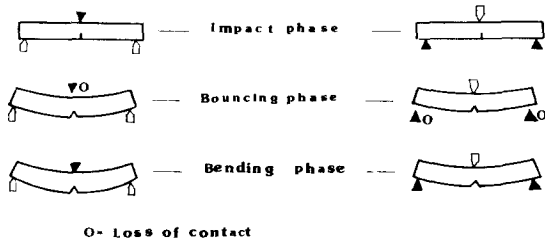


Fig. 6 The three phases; Model 1 to the left and model 2 to the right

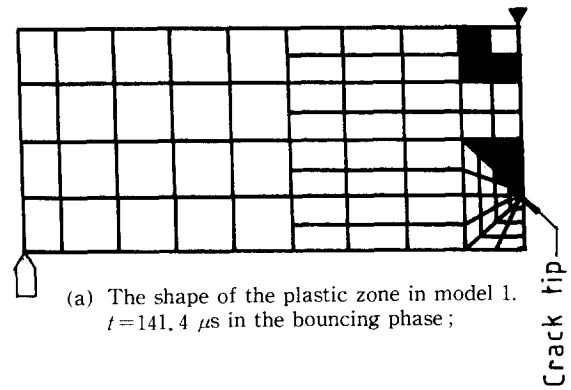
because only half the specimen is regarded at the FEM analysis.

Immediately after impact F_{1B} increases rapidly to about 70 KN and reaches about 97 KN. After about 28 μs the stress wave reaches the support point A, where a small value of F_{1A} is induced during about 10 μs . The specimen then loses contact with the support point at A. The maximum gap opening displacement is about 0.094 mm after 103 μs . 174 μs after impact, the midpoint gap again closes and F_{1A} increases. F_{1A} grows rapidly to about 20 KN and increases thereafter approximately linearly with time. F_{1B} shows damped oscillations with a period of about 150 μs (this period is reduced slightly with increasing time). At the end of the simulation, the magnitudes of the force at the load and support points are almost the same. As shown later, the specimen behavior approaches a quasi static state.

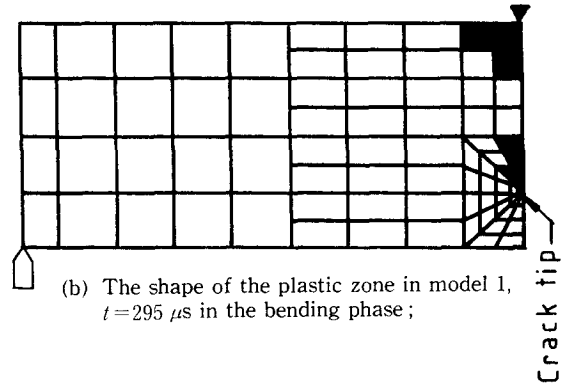
4.2 The Deformation and Reaction Force in Model 2

The diagram for reaction forces at the middle point A and side point B and gap opening displacement at point B for model 2 is shown in Fig. 5.

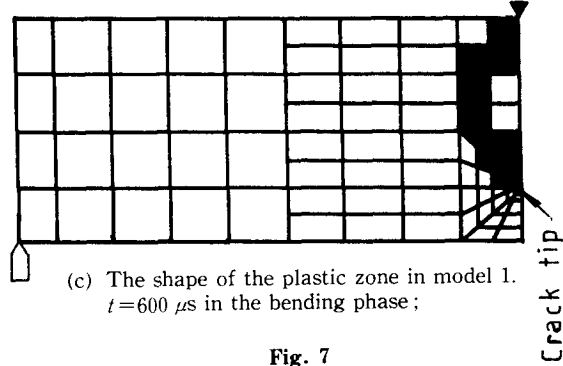
The specimen is hit at the middle point and the force at the load point increases rapidly to about 20 KN. F_{2A} then increases to about 56 KN. About 28 μs after impact, the stress wave reaches the support point B. A small value of F_{2B} is induced for about 10 μs . Thereafter, the gap element at B opens and remains opened until about 148 μs is reached. Maximum gap opening displacement is about 0.029 mm and it



(a) The shape of the plastic zone in model 1.
 $t = 141.4 \mu s$ in the bouncing phase ;



(b) The shape of the plastic zone in model 1,
 $t = 295 \mu s$ in the bending phase ;



(c) The shape of the plastic zone in model 1.
 $t = 600 \mu s$ in the bending phase ;

Fig. 7

occurs after about 95 μs . F_{2A} increases approximately linearly with time until the gap element closes at the support point. However, F_{2B} shows markedly damped oscillations with a period similar to the one in model 1. As in model 1, the forces at the load point and at the support point approach the same value, which is about the same as in model 1, namely about 50 KN.

4.3 Three Phases and Similarities in the Dynamic Response

A comparison between model 1 and model 2 has been made and it is shown that they behave essentially in the same way. A qualitative division into three different phases, which are named uniquely in this paper, can be made according to Fig. 6.

For both models, the force at the load point reaches very high values immediately after impact. After about 28 μs , the first stress wave reaches the support point, at which a small reaction force is induced. At about 40 μs after impact, the gap element at the support point opens. This period, from impact

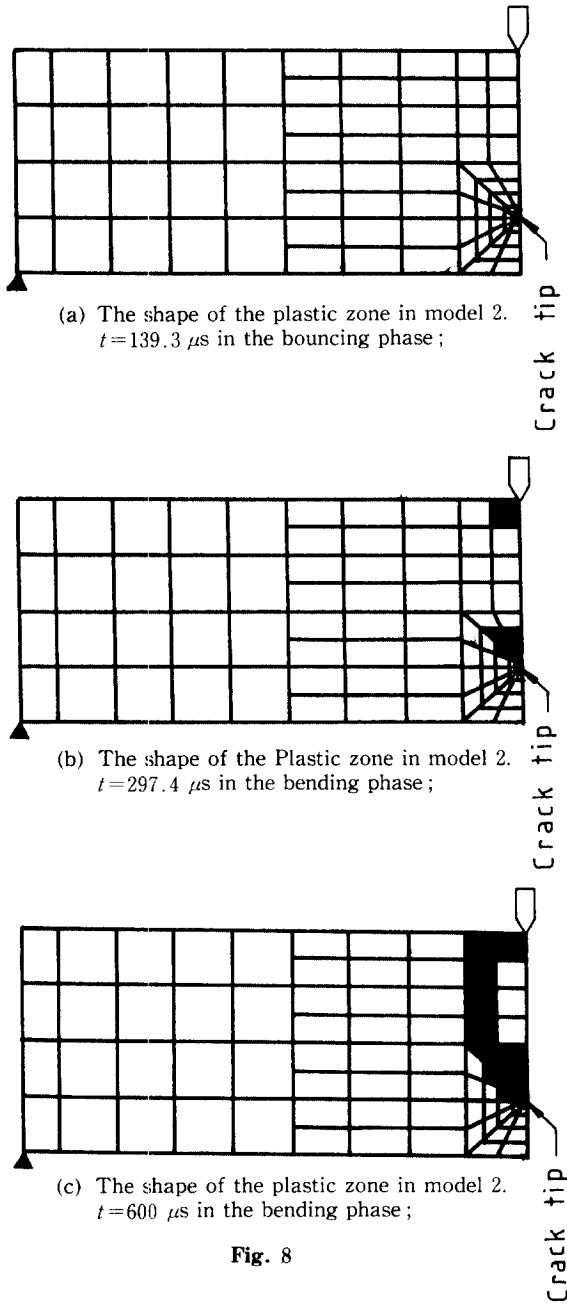


Fig. 8

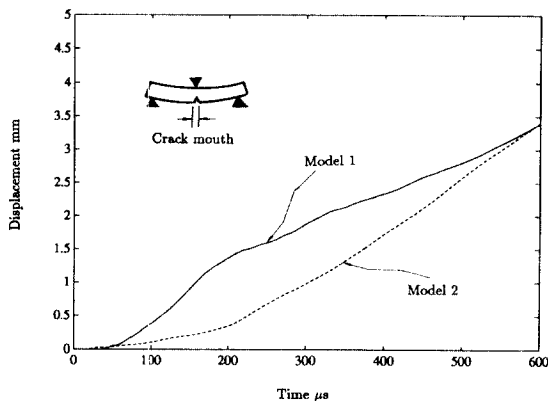


Fig. 9 Crack mouth opening displacement history

up to approximately $40 \mu s$, is named as the “impact phase.” No plastic deformation near the crack tip is found before $40 \mu s$ in both of the two models. The second phase is called the “bouncing” phase and this phase is sustained until the gap element at the support point closes again. During this phase, the specimen is found to be deformed as a free supported beam by the inertia. This effect was also observed in the experimental investigations (W. Bohme, 1982 and Kalthoff, 1985). The gap opening displacement at the support point as well as the reaction force at the load point for model 1 is about 3 times larger than that in model 2.

Examples of the plastic zone shape during the bouncing phase are shown in Fig. 7(a) and Fig. 8(a) for model 1 and for model 2, respectively. The plastic zone size is found to grow during the bouncing phase. The third phase is named as “bending phase.” This phase starts, as mentioned above, when the gap at the support point closes and reaction force rapidly increases. Fig. 7(b) and Fig. 8(b) show the plastic zones at about $300 \mu s$ in the two models. The areas of the plastic zones in the vicinity of the crack tip and adjacent to point A are found to grow. The mechanical behavior may be characterized by damped oscillations and at the end of this phase, an approximately quasi static state is reached. The reaction force at the side point oscillates around the stable middle point reaction force. The oscillation of the side point force is damped out and approaches the middle point reaction force (about 50 KN) at the end of simulation. Fig. 7(c) and Fig. 8(c) show the plastic zones at $600 \mu s$ in two models. The plastic zones at the middle point A and at the crack tip are linked together by plastic hinge (see Fig. 7(c) and Fig. 8(c)). Figure 9 shows the variation of crack mouth opening displacement with respect to times.

During the impact phase, the crack mouth opening displacements in both models are almost zero. During the bouncing phase, the maximum value of the gap opening displacement at the support point in model 1 is about three times larger than the corresponding value in model 2. The crack mouth opening displacement is also larger in model 1 as compared to that in model 2.

5. THE STATIONARY BEHAVIOR OF MODEL 1 AND MODEL 2

In order to investigate the overall behavior of the specimen, additional calculations covering the period up to $1800 \mu s$ have been performed without considering crack propagation. Some of the results are shown in Figs. 10, 11, and 12. The forces at points A and B and the crack mouth opening displacement have been calculated and compared to the quasi static case in order to investigate the stationary behavior of the two models. The quasi static calculations are performed by enforcement of a displacement $d = V * t$ at point A. As expected, the magnitudes of the forces for both models approach the same value with increasing time. After about $1000 \mu s$, both midpoint reaction forces practically approach the quasi static value as shown in Fig. 10. The reaction forces at the side point show damped oscillations and approach the quasi static value as seen in Fig. 11. At this time, the crack mouth opening displacement exhibits differences between the two models, see Fig. 12. After the impact, this displacement in model 1 is clearly larger than that in model 2. After $600 \mu s$, the displacement is nearly the same in both model 1 and 2. But these displacements are found to be smaller than that of

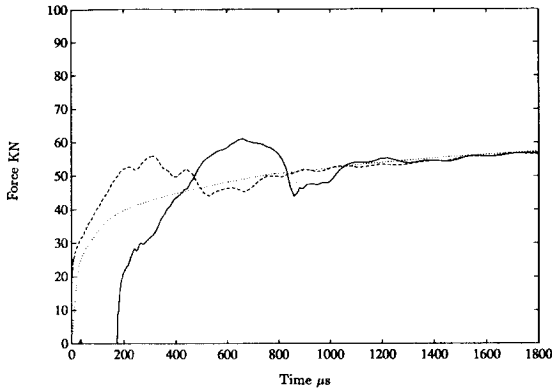


Fig. 10 The reaction force at point A. Up to 1800 μ s after impact Model 1 : solid line ; Model 2 ; dashed line ; Quasi static case : dotted line

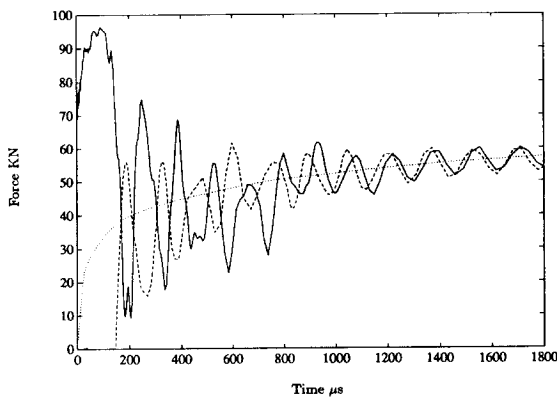


Fig. 11 The reaction force at point B. Up to 1800 μ s after impact Model 1 : solid line ; Model 2 ; dashed line ; Quasi static case : dotted line

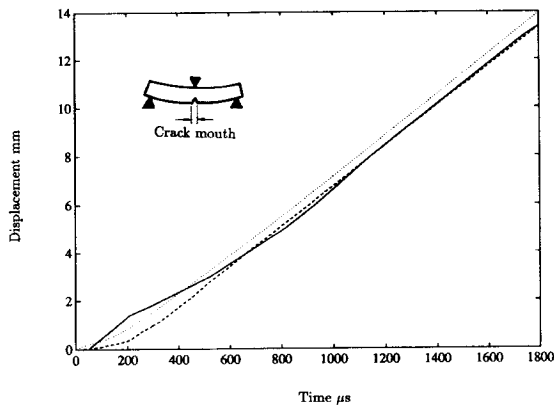


Fig. 12 The crack mouth opening displacement. Up to 1800 μ s after impact Model 1 : solid line ; Model 2 : dashed line ; Quasi static case : dotted line

quasi static case.

6. CONCLUSION

For two different impact loading conditions in three point

bend specimen models (model 1 : impact at the side points, model 2 : impact at the middle point), three distinct phases are found by using dynamic finite element method. The events during these three phases are similar in the two models and, in principle, the behavior of the two models seems to be the same. The three phases may be characterized as follows ;

(1) Phase one : impact phase. The specimen is impacted and during this phase the first stress wave reaches the support point. This results in loss of contact between the specimen and the support roller.

(2) Phase two : bouncing phase. The specimen is bounced away from the support roller and back again. The plastic zone in the vicinity of the crack tip starts to form and grows.

(3) Phase three : bending phase. The oscillation is damped out and approaches the middle point reaction force (about 50KN) at the end of simulation.

(4) The time to develop the plastic zone which terminates in a plastic hinge does not seem to be dependent on whether the impact occurs at the middle point or occurs at the side point.

(5) The reaction forces in both model 1 and model 2 show damped oscillations and approach the quasi static case.

ACKNOWLEDGEMENT

This study was supported by KOSEF (Korea Science and Engineering Foundation).

REFERENCES

- ABAQUS manual, 1989, Version 4.8, Hibbit, Karlsson and Sorensen, Inc.
- Ahmad, J., Jung, J., Barnes, C.R. and Kanninen, M.F., 1983, "Elastic-Plastic Finite Element Analysis of Dynamic Fracture," *Eng. Frac. Mech.*, Vol.17, No.3, pp.235~246.
- Kalthoff, J.F., 1983, "On Some Current Problems in Experimental Fracture Dynamics," Workshop on Dynamic Fracture, Knauss W.G., Ravichandar and Rosakis A.J. (eds.), pp.11~35.
- Kalthoff, J.F., 1985, "On the Measurement of Dynamic Fracture Toughness a Review of Recent Work," *Int. Jour. of Frac.*, Vol.27, pp.277~298.
- Kanninen, M.F., Gehlen, P.C., Barnes, C.R., Hoagland, R.G. and Hahn, G.T., 1979, "Dynamic Crack Propagation under Impact Loading," *Nonlinear and Dynamic Fracture Mechanics*, Perrone N. and Atluri S.N. (eds.), ASME AMD 35, pp. 185~200.
- Rosakis, A.J., Zehnder A.T., and Narasimhan, R., 1988, "Caustics by Reflection and their Application to Elastic-Plastic and Dynamic Fracture Mechanics," SPIE Conference on Photomechanics and Speckle Metrology, San Diego, California.
- Van Elst, H.G., 1984, "Assessment of Dynamic Fracture Propagation Resistance at Instrumented High Velocity Gas-gun Impact Tests on SENB-Specimens," *ICF 6*, Vol.5, pp.3089~3097.
- Wihlborg, G., 1985, "Design and Application of a Rig for High Energy Impact Tests," IUTAM Symposium Tokyo/Japan.
- Bergmark, A. and Kao, H.R., 1991, "Dynamic Crack Initiation in 3PB Ductile Steel Specimens," Technical Report LUTFD 2, TFHF 3041, Lund, Sweden.